Relationship Between the Barrier Layer Thickness and Upper Ocean Heat Content in the Western Tropical Pacific Ocean

Sry Wei

University of Washington

School of Oceanography, Box 357940

Seattle WA 98195-7940

wei77@uw.edu

Abstract

Barrier layers form when density-defined mixed layer is shallower than the temperature-defined isothermal layer. It can reduce vertical mixing and entrainment cooling, influencing upper-ocean heat storage. This study examines barrier layer variability near the Mariana Trench using 43 independent underway CTD profiles collected from the R/V *Thomas G. Thompson* during 27–28 March 2026, together with ERA5 reanalysis surface forcing data. Barrier layer thickness was calculated from vertically binned temperature, salinity, and density profiles. Upper-ocean heat content was integrated over 0–200 m for profiles with sufficient depth coverage, and precipitation, precipitation – evaporation (P – E), wind speed, and wind stress were matched to each profile over 1-, 6-, 12-, and 24-h windows. Barrier layers were common but spatially heterogeneous. The zonal East transect had the thickest and most persistent barrier layers, while the meridional transect showed a sharp transition from thin to thick barrier layers over kilometer-scale distances. Precipitation and P − E were weakly correlated with barrier layer thickness, whereas wind stress showed a stronger negative linear relationship, especially over 24-h window ($r = -0.524$, $p < 0.001$). Barrier layer thickness showed a weak positive relationship with upper-ocean heat content ($r = 0.223$, $p = 0.156$), but the correlation was not statistically significant. Thus, the hypothesis that thicker barrier layers are associated with greater fixed-depth upper-ocean heat content was partially supported but not statistically confirmed. This suggests that thicker barrier layers may help retain heat, but BLT alone did not explain fixed-depth upper-ocean heat content in this short cruise-based dataset.

Plain Language Summary

The western tropical Pacific often has a warm upper ocean, but how the heat is stored depends on both salinity and temperature structures. A barrier layer forms when changes in salinity make the surface ocean strongly layered, even though temperature stays warm to deeper depths. This structure can reduce vertical mixing between surface water and cooler deep water, which may help heat remain in the upper ocean.

In this thesis, I used ship-based ocean measurements during March 2026 and weather data to test whether thicker barrier layers were linked to stronger heat storage near the Mariana Trench. The observations showed that barrier layers were common but highly variable. The east side of the Mariana Trench had many thick barrier layers, while one north-south transect showed a sharp change from thin to thick layers over only a few kilometers. Recent rainfall did not show a clear relationship with barrier layer thickness, but weaker wind stress was more often associated with thicker barrier layers. Thicker barrier layers were weakly associated with higher upper-ocean heat content, but the relationship was not strong enough to confirm the hypothesis. Overall, these results suggest that barrier layers may help influence heat retention, but local temperature structure, differences among water masses, and short-term sampling limitations also matter.

Introduction

Marine heatwaves (MHW) are climate extremes that can significantly affect ecosystems and human society through coral bleaching, hypoxia, harmful algal blooms, ecosystem restructuring, and losses in aquaculture and fisheries (Couch et al., 2017; Hobday et al., 2016). Tropical marine heatwaves have also been linked to severe ecological impacts in warm-water regions, including extreme warming events across tropical Australia (Benthuysen et al., 2018). MHWs are commonly defined as a prolonged period of anomalously warm conditions for at least five consecutive days in the ocean (Hobday et al., 2016). Their development and persistence are influenced by atmospheric forcing and ocean feedbacks, including large-scale climate variability such as El Niño–Southern Oscillation (ENSO). The vertical structure of the upper ocean modulates the storage, mixing, and redistribution of heat. In particular, the depth of the mixed layer determines the volume of water over which surface heating is distributed and controls the entrainment of cooler subsurface waters.

One important feature of the upper ocean is the barrier layer, defined as the layer between the isothermal layer and the mixed layer (Lukas & Lindstrom, 1991). A barrier layer forms when salinity stratification is strong enough to make density-defined mixed layer shallower than the temperature-defined isothermal layer, while temperature remains relatively uniform to a greater depth. This produces a positive barrier layer thickness as illustrated by an observed uCTD profile from our data (Fig. 1). The presence of a barrier layer can inhibit entrainment cooling by isolating the mixed layer from the cooler thermocline waters below. Water within the barrier layer can have nearly the same temperature as the mixed layer but higher salinity, resulting in slightly higher density and suppressed vertical mixing. As a result, barrier layers may help maintain warm upper-ocean conditions by trapping heat within a shallower layer.

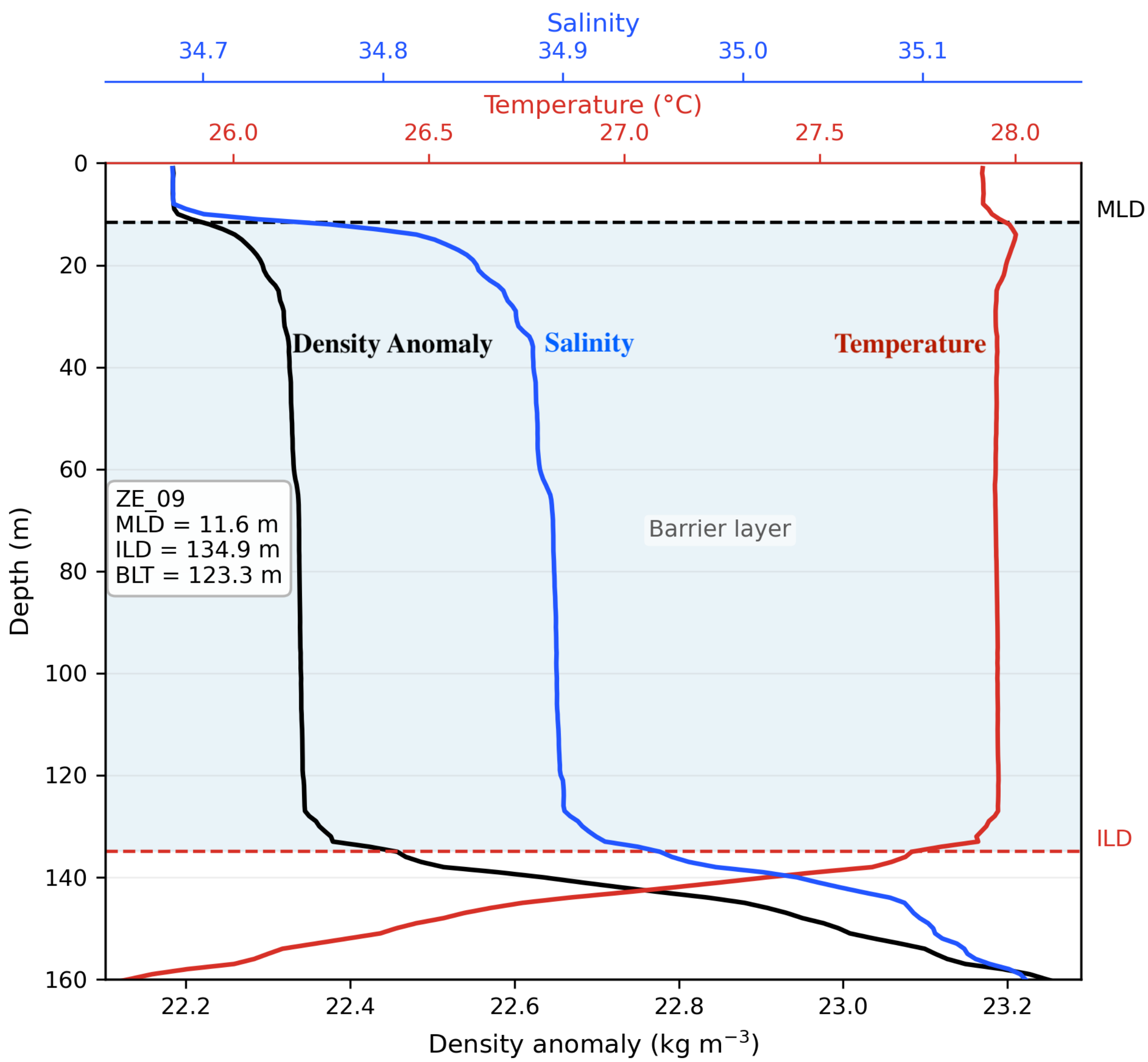

Figure 1. Observed uCTD example of a thick barrier layer (> 30 m). Vertical profiles of density anomaly, temperature, and salinity are shown for profile ZE_09. The density-defined MLD and temperature-defined ILD are marked by dashed horizontal lines. The shaded region between MLD and ILD represents the BL.

Barrier layer thickness (BLT) varies with different local surface forcing and large-scale ocean dynamics. Weak surface wind stress can reduce turbulent mixing, while heavy precipitation can introduce buoyant freshwater that strengthens near-surface salinity stratification and makes the density-defined mixed layer shoal relative to the isothermal layer. Horizontal advection of salinity fronts, Ekman-driven tilting of salinity gradients, vertical shear in surface currents, and large-scale climate variability such as ENSO can also contribute to barrier layer formation and variability (Bosc et al., 2009; Katsura & Sprintall, 2020; Zhang et al., 2021). The western Pacific warm pool is a region where these processes frequently occur and are particularly active, because warm upper-ocean temperatures and strong salinity stratification frequently support thick and seasonally varying barrier layers (Bosc et al., 2009; Lukas & Lindstrom, 1991).

The Mariana Trench lies within the western Pacific warm pool, where barrier layers are commonly observed and the upper-ocean stratification can influence heat storage. Previous work has documented climatological barrier layer variability in the western Pacific warm pool and has shown that barrier layers can be linked to precipitation, wind forcing, salinity stratification, and large-scale climate variability (Bosc et al., 2009; Zhang et al., 2021). However, less is known about how short-term, profile-scale variations in BLT relate to recent surface forcing and fixed-depth upper-ocean heat content near the Mariana Trench. This study provides a useful local, cruise-based perspective because shipboard profiles can resolve small-scale vertical structure that may be smoothed in broader climatological products.

This study examines the occurrence and variability of barrier layer near the Maraina Trench using ship-based underway conductivity–temperature–depth (uCTD) observations and ERA5 reanalysis data. The main objectives are to investigate BLT variability across sampling transects (Fig. 2), evaluate whether recent precipitation and wind stress are associated with BLT, and test whether thicker barrier layers are associated with greater OHC within a fixed 0–200 m layer. I hypothesize that thicker barrier layers are associated with greater fixed-depth OHC, consistent with enhanced stratification and reduced vertical mixing in response to surface forcings. By linking BLT variability to surface forcing and OHC across the sampling sites, this study may contribute to understanding how salinity-driven stratification may influence upper-ocean thermal structure in the western tropical Pacific.

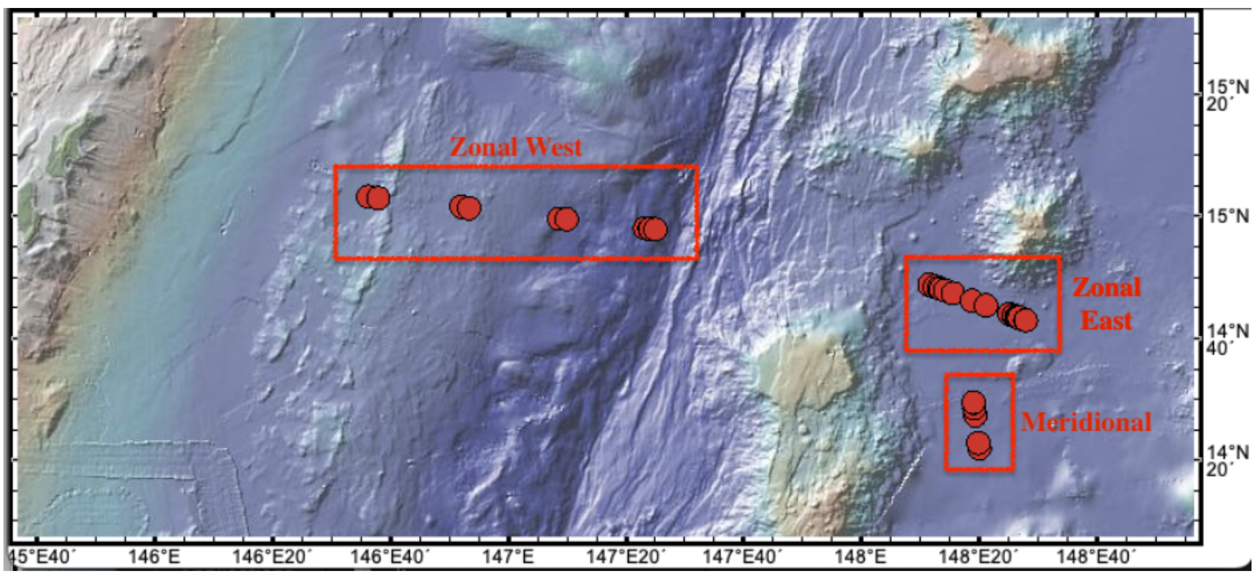

Figure 2. uCTD sampling sites from the R/V Thomas G. Thompson during 27–28 March 2026. The two zonal transect groups are located west and east of the Mariana Trench, and the meridional transect group is located east of the trench.

Methods

Field sampling and uCTD observations

Underway conductivity–temperature–depth (uCTD) profiles were collected during the University of Washington School of Oceanography Senior Cruise aboard the R/V *Thomas G. Thompson* near Guam and the Mariana Trench from 27–28 March 2026. The sampling design included one sparse zonal transect on the west of the Mariana Trench, one higher-resolution zonal transect on the east of the trench, and one meridional transect on the east side of the trench (Fig. 2). Based on the cruise plan and profile locations, the sampling region covered approximately 14.3–15.1°N and 146.5–148.6°E.

The uCTD casts were collected using an RBRconcerto³ CTD probe. The probe measured pressure, temperature, and conductivity, from which salinity and density-related variables were derived during post-processing. Casts were aimed to sample the upper 300 m of the ocean to resolve the mixed layer, isothermal layer, barrier layer, and upper-ocean thermal structure. During uCTD deployments, the ship was slowed to approximately 4–5 kt. For repeated high-resolution casting, the probe was soaked on the surface for more than 10s, released for approximately 3–3.5 min to sample the upper 300 m, recovered with the reel, and then redeployed after a short waiting period when conditions allowed.

The spatial resolution differed among transects. The zonal transects were sampled more sparsely (approximately 20-25 km) because the ship transit distance is more than 140 km when crossing the Mariana Trench. Based on the cruise plan, these casts were deployed approximately hourly during part of the west-to-east transit, as the ship moved at about 11.5 kt during transit and slowed to 4.5 kt to complete each double-drop uCTD deployment. In contrast, the meridional transect was sampled at higher resolution during slower mapping with repeated underway casting. For the meridional multiple-drop profiles, adjacent downcasts were separated by approximately 10–11 min at a ship speed of about 4.5 kt, corresponding to an approximate spacing of 1.4–1.5 km. The final profile locations were treated as the primary record of sampling position.

uCTD profile processing

The uCTD profiles used in this thesis were processed from CSV files provided by Professor Gray. These files include sea pressure, temperature, salinity, density anomaly, potential temperature, absolute salinity, and cast direction. When both downcast and upcast data were available, the downcast portion was used because it is generally less affected by uneven pull-up speed, wire motion, and reel effects during recovery. Each profile was screened to remove missing or nonphysical values, and the remaining observations were vertically binned into 1 dbar bins. Because the profiles were collected in the upper ocean, pressure in dbar was treated as approximately equivalent to depth in meters.

After binning, each profile was checked for sufficient vertical coverage and for duplicated or aliased processed files. Duplicate or aliased profiles were identified by comparing maximum binned depth, MLD, ILD, and BLT values rounded to 0.1 m, with one-to-one matching between timestamp-based and station-based filenames. One file from each duplicate pair was retained. After this screening, 43 independent profiles were used for the main BLT analysis, including 15 zonal West, 18 zonal East, and 10 meridional profiles. The duplicate screening results are documented in Table A2, and the final independent profile list is provided in Table A1.

MLD, ILD, BLT, and OHC

MLD was calculated using the threshold method described by de Boyer Montégut et al. (2004). Specifically, MLD is defined as the depth at which potential density increases by $\Delta\sigma_{\Theta} = 0.03$ $kg\ m^{-3}$ relative to its value at 10 m depth. The 10 m reference depth is chosen to reduce the influence of short-term surface variability and diurnal warming. This density threshold has been used in studies of barrier layer variability in the western Pacific warm pool (e.g., Bosc et al., 2009) and is consistent with the density-based definition of MLD applied in classic barrier layer studies (e.g., Lukas & Lindstrom, 1991). Since Guam is located within the western Pacific warm pool region, adopting the same density criterion helps maintain consistency in methodology and allows comparison with previous studies in similar environments.

The ILD was defined as the depth at which the temperature decreases by 0.2°C relative to its value at 10 m depth. When the ILD is deeper than MLD, barrier layer thickness (BLT) was then calculated as:

$$BLT = ILD - MLD$$

BLT values were grouped into three descriptive classes: thin BLs were defined as BLT < 10 m, moderate BLs as 10–30 m, and thick BLs as BLT ≥ 30 m. These thresholds were used only to organize and compare profile structure across transects and figures. They are not treated as universal barrier layer categories; the physical BLT values and continuous correlations are used for the main quantitative analysis.

OHC was calculated for independent BL-resolved uCTD profiles that extended to at least 200 m. Temperature profiles were vertically binned to 1 m resolution, and heat content was integrated over a fixed 0–200 m layer as:

$$OHC = \rho c_p \int_{0\,m}^{200\,m} T(z)\, dz$$

, where ρ = 1025 $kg\ m^{-3}$is the seawater density, $c_p\ = 3992\ J\ kg^{-1}\ ºC^{-1}$ is the specific heat capacity, and T(z) is the in situ temperature. OHC values were converted from $J\ m^{-2}$to $GJ\ m^{-2}$. Profiles that did not reach 200 m were excluded from the primary OHC analysis. As a robustness check, OHC was also calculated over 10–200 m to test whether the BLT–OHC relationship was controlled by the uppermost 10 m (Table A5).

ERA5 surface forcing data

Surface forcing was examined using ERA5 Reanalysis hourly data on single levels from the Copernicus Climate Change Service Climate Data Store. ERA5 is the fifth-generation ECMWF reanalysis product and provides hourly global estimates of atmospheric, land-surface, and ocean-wave variables by combining observations with model output through data assimilation. The CDS ERA5 single-level product is provided on a regular latitude–longitude grid, with a 0.25° × 0.25° atmospheric resolution, hourly temporal resolution, and temporal coverage from 1940 to present (Hersbach et al., 2023).

ERA5 data were downloaded over a regional box of 13.25–16°N and 144–149°E, covering the cruise sampling stations (Fig. 2). Six ERA5 variables were used: 10 m u-wind component, 10 m v-wind component, evaporation, total precipitation, mean eastward turbulent surface stress, and mean northward turbulent surface stress. The 10 m u- and v-wind components represent the eastward and northward wind components at 10 m above the surface and have units of $m\ s^{-1}$. Wind speed was calculated from these two components as:

$$U_{10} = \sqrt{u_{10}^2 + v_{10}^2}$$

where u_{10} and v_{10} are the 10 m eastward and northward wind components.

Total precipitation represents hourly accumulated precipitation depth in meters. Evaporation is provided as accumulated water-equivalent depth; in ERA5, evaporation from the surface to the atmosphere is defined with a negative sign, so the sign convention was checked before calculating precipitation minus evaporation. In this thesis, total precipitation and evaporation were converted to millimeters and used to calculate freshwater forcing. A precipitation-minus-evaporation estimate was calculated as P−E, where positive values represent net freshwater input to the ocean surface.

Mean eastward and northward turbulent surface stress represent the two horizontal components of turbulent momentum flux at the surface, with units of $N\ m^{-2}$. Wind stress magnitude was calculated as:

$$\tau = \sqrt{\tau_x^2 + \tau_y^2}$$

where τ_x is the eastward turbulent surface stress and τ_y is the northward turbulent surface stress.

ERA5 variables were matched to each uCTD profile using the profile time and position. For each profile, precipitation and P − E were accumulated over 1-, 6-, 12-, and 24-h windows before the profile time. Wind speed and wind stress magnitude were averaged over the same time windows

(Table A3). These matched forcing values were then compared with BLT to evaluate whether recent surface forcing was associated with observed barrier layer variability.

Statistical analysis

The relationships between BLT, ERA5-derived surface forcing, and OHC were evaluated using Pearson and Spearman correlation coefficients. Pearson correlation was used to describe linear association, while Spearman correlation was used to describe rank-based monotonic association. Both metrics were included because the dataset was small and transect structure could produce relationships that were not strictly linear. Two-sided p-values were calculated for each correlation coefficient and were used to evaluate whether the observed correlations were distinguishable from zero at the 0.05 significance level.

The correlations were interpreted as descriptive statistics rather than causal tests. This is because the dataset contained a limited number of independent profiles, the transects had uneven spatial resolution, and neighboring repeated profiles were not fully independent in space. In addition, Pearson correlation assumes an approximately linear relationship and can be influenced by group structure or outlying values, while Spearman correlation tests only whether the rank order of two variables changes together. Therefore, the statistical analysis was used to identify observational patterns and compare variables, not to establish causality.

Results

Barrier Layer

Barrier layers were calculated from the processed uCTD profiles using the density-defined MLD and temperature-defined ILD described in the Methods section. A total of 55 post-processed uCTD profiles were screened, and 12 were identified as duplicate or aliased files by comparing maximum binned depth, MLD, ILD, and BLT values rounded to 0.1 m (Tables A1–A2). After one file from each duplicate pair was removed, 43 independent profiles were retained for the main BLT analysis, including 15 zonal West, 18 zonal East, and 10 meridional profiles (Table 1).

Table 1. Summary of MLD, ILD, and BLT by transect group with profile numbers and BL categories.

Transect group	**Number of Independent profile**	**MLD median & range (m)**	**ILD median & range (m)**	**BLT median & range (m)**	**BL class counts thin/moderate/thick**
zonal West	15	27.3 (10.6–96.0)	107.6 (81.2–122.1)	70.3 (7.7–102.5)	1/4/10
zonal East	18	19.9 (11.6–121.9)	124.3 (100.3–142.5)	102.1 (1.7–124.5)	3 / 0 / 15
meridional	10	15.5 (11.9–33.0)	19.4 (13.6–137.3)	4.3 (0.3–119.6)	6 / 0 / 4

Note: MLD, ILD, and BLT are defined in the Methods section. Values were calculated from independent uCTD profiles after duplicated or aliased processed files were removed to avoid counting the same physical profile more than once. Values in parentheses indicate the range. Thin, moderate, and thick barrier layers are defined as BLT <10 m, 10–30 m, and ≥30 m, respectively.

BLT varied strongly among transect groups. The zonal East group had the largest median BLT and the greatest number of thick BL cases, with 15 of 18 profiles classified as thick BLs. The zonal West group also contained many thick BLs but showed a wider range of BLT values, including thin, moderate, and thick cases. The meridional group had the lowest median BLT but the strongest contrast between thin and thick BL cases, with six thin BL profiles and four thick BL profiles (Table 1). Across all independent profiles, BLT ranged from 0.3 to 124.5 m.

Profile-level BLT patterns show that these transect differences were not evenly distributed along each transect. In the zonal West group, BLT generally increased from thinner and moderate values in the earlier profiles to mostly thick BL values in ZW_08–ZW_15. In the zonal East group, ZE_01–ZE_03 were thin BL cases, while ZE_04–ZE_18 were all thick BL cases. In the meridional group, M_01–M_05 and M_10 were thin BL cases, while M_06–M_09 were thick BL cases (Fig. 3; Table A1). The transition from M_05 to M_06 occurred over one adjacent-profile spacing of approximately 1.4–1.5 km, showing that BLT changed sharply over kilometer-scale spacing along the meridional transect.

Representative profiles show the vertical structure associated with thin and thick BL cases (Fig. 4). In the selected thin BL examples, MLD and ILD were separated by only a few meters. In the selected thick BL examples, MLD remained shallow while ILD extended to approximately 100–140 m, producing BLT values greater than 100 m in ZW_15, ZE_09, and M_08. The full set of independent profile panels is provided in Figs. A1–A3, with profile-level values listed in Table A1.

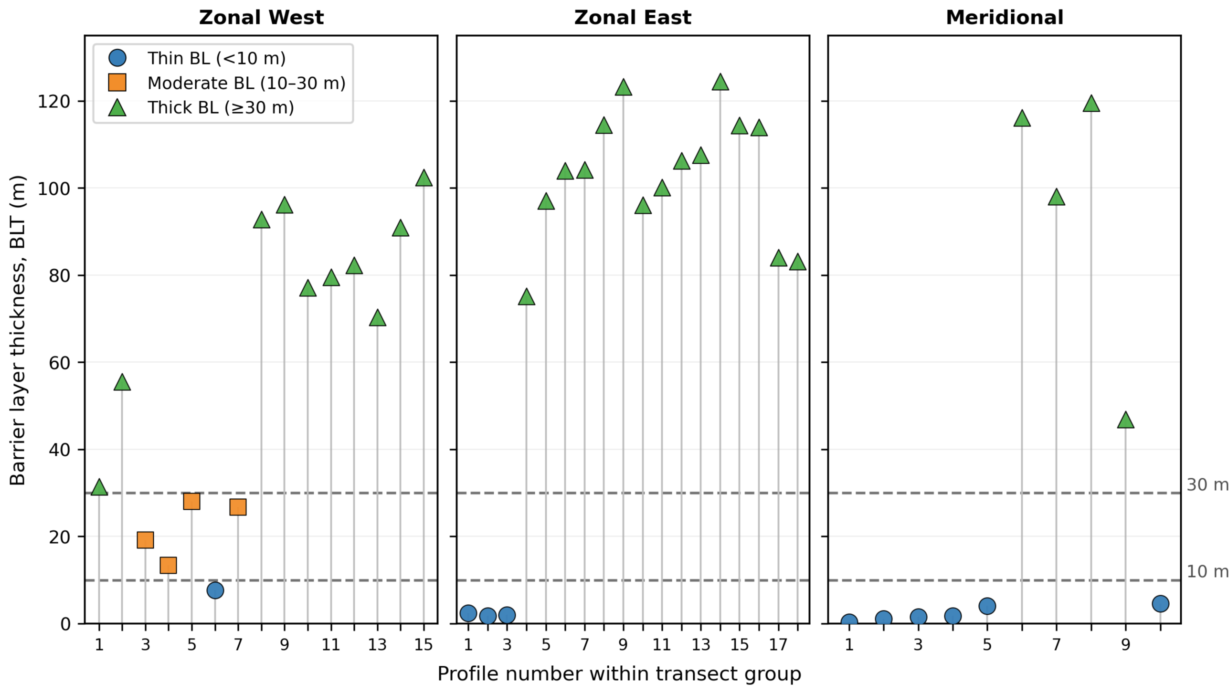

Figure 3. Barrier layer thickness by transect group. Each point represents one independent uCTD profile after duplicated or aliased processed files were screened. Marker colors and shapes indicate thin BL (<10 m), moderate BL (10–30 m), and thick BL (≥30 m). Dashed horizontal lines mark the 10 m and 30 m thresholds used for the descriptive BL classes. X-axis numbers indicate profile order within each transect group.

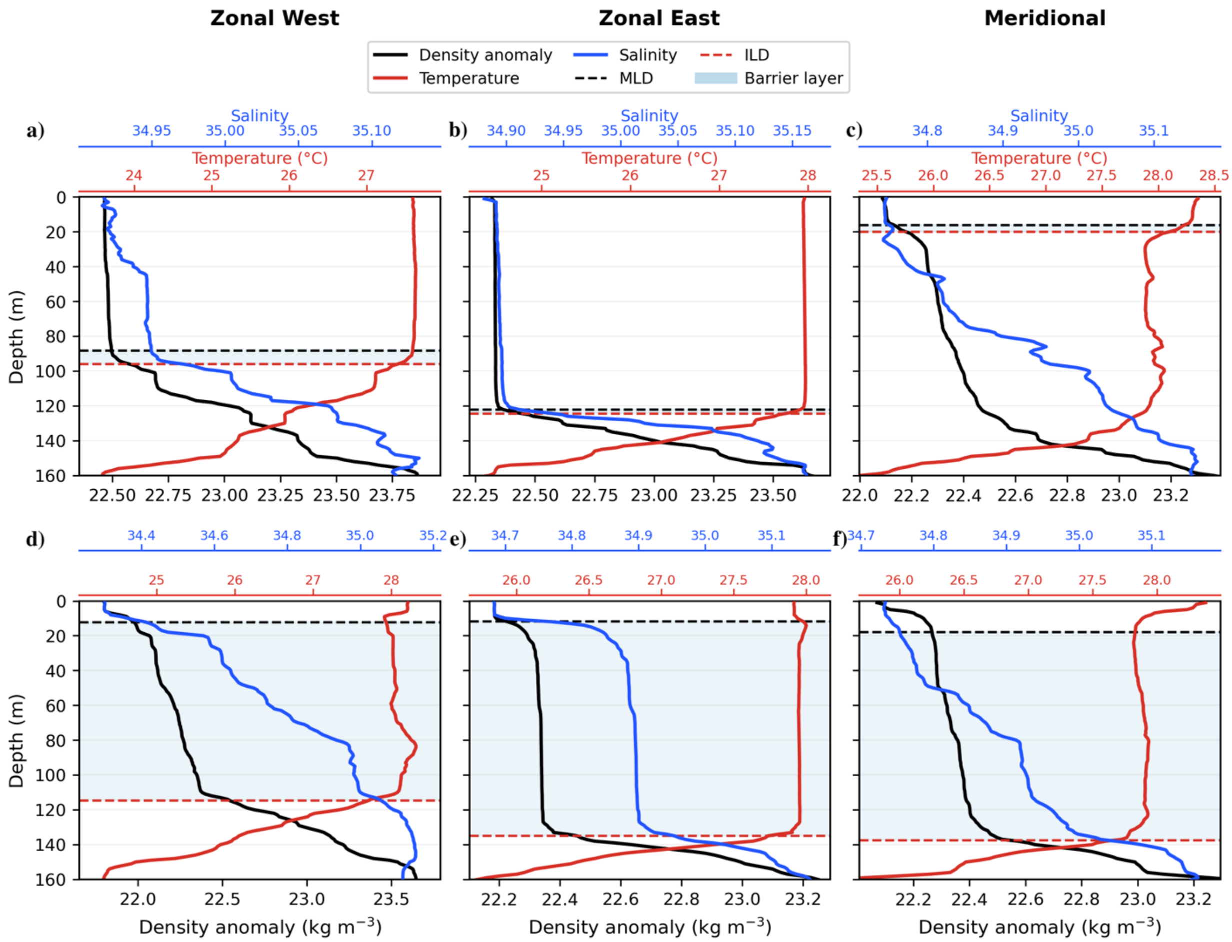

Figure 4. Selected representative uCTD profiles showing thin and thick BL cases. Black curves show density anomaly, red curves show temperature, and blue curves show salinity. The lower x-axis is density anomaly, the red upper x-axis is temperature, and the blue upper x-axis is salinity. The black dashed line marks MLD, the red dashed line marks ILD, and blue shading marks the barrier layer between MLD and ILD. Thick barrier layers occur where the density-defined MLD remains shallow while the temperature-defined ILD extends much deeper.

Barrier Layer Thickness and Surface Forcing

ERA5-derived precipitation, P − E, wind speed, and wind stress were compared with BLT over 1-, 6-, 12-, and 24-h windows before each profile. Precipitation-related variables showed weak correlations with BLT across all time windows (Fig. 5a–b; Table A3). For total precipitation, Pearson correlations were near zero except for a weak positive 1-h correlation, and all precipitation p-values were greater than 0.05. Spearman correlations for precipitation were weakly negative across all windows. P − E showed a similar pattern, with weak Pearson and Spearman correlations and no statistically significant relationships (Table A3).

Wind stress showed the strongest surface-forcing signal. Pearson correlations between BLT and mean wind stress were negative for all time windows and were statistically significant for the 6-, 12-, and 24-h windows (Fig. 5c; Table A3). The strongest Pearson correlation occurred over the 24-h window ($r = -0.524$, $p < 0.001$). In contrast, Spearman correlations for wind stress were weaker and were not statistically significant (Fig. 5d; Table A3). Wind speed showed a similar but slightly weaker pattern, with the 24-h Pearson correlation equal to −0.436 ($p = 0.003$), while Spearman correlations remained weak (Table A3).

The profile-level 24-h forcing values show the range of surface conditions sampled during the cruise. Across the 43 independent profiles, 24-h precipitation ranged from 0.57 to 40.17 mm, 24-h P − E ranged from −2.28 to 37.50 mm, 24-h mean wind speed ranged from 2.11 to 10.11 $m\ s^{-1}$, and 24-h mean wind stress ranged from 0.0076 to 0.1598 $N\ m^{-2}$ (Table A4). Overall, precipitation and P − E showed weak relationships with BLT, whereas wind stress had the strongest negative Pearson correlation, particularly over the 24-h window.

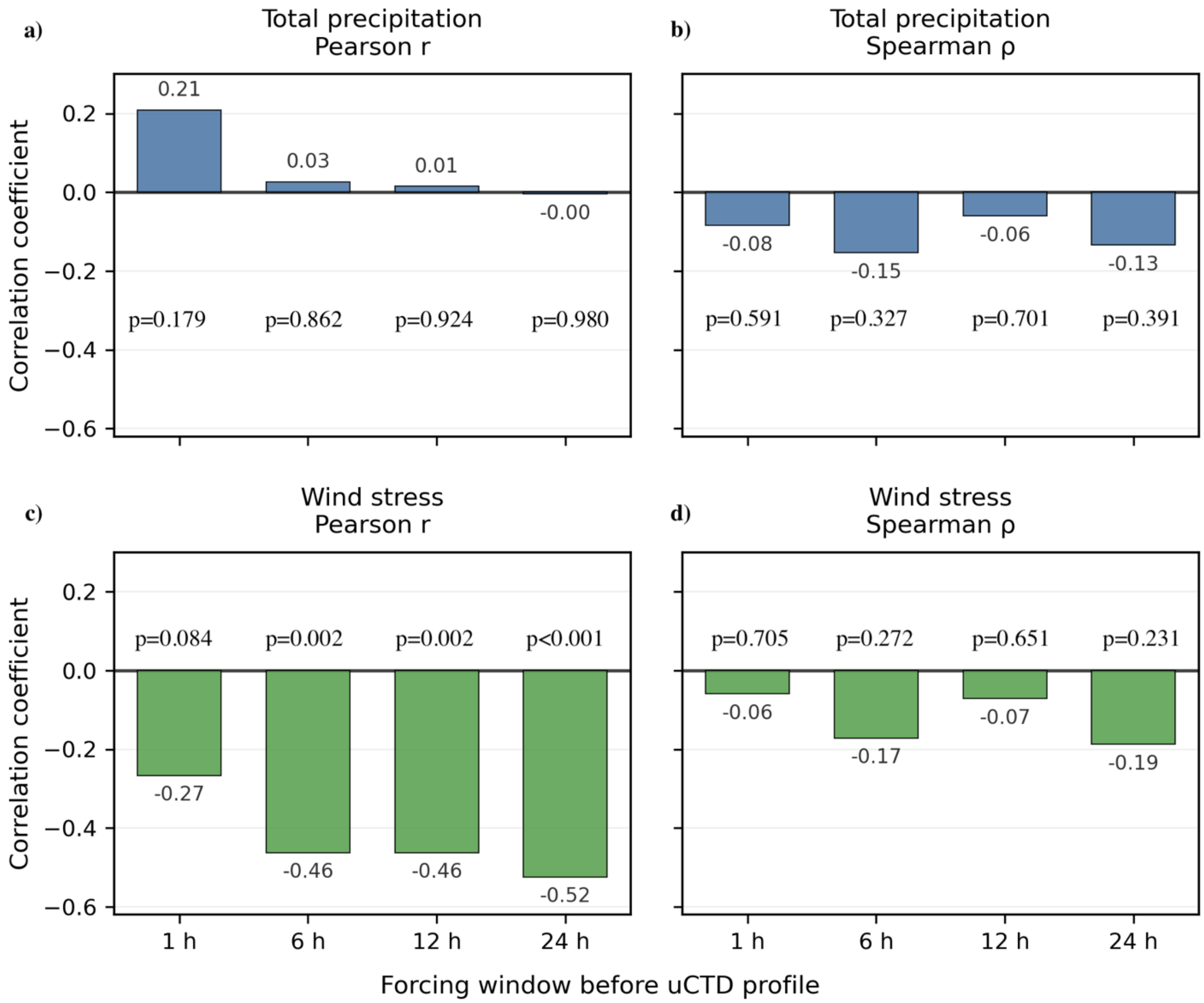

Figure 5. Correlations between BLT and ERA5-derived precipitation and wind stress across different forcing windows. Pearson r and Spearman ρ correlation coefficients were calculated between BLT and ERA5-derived surface forcing variables for 43 independent uCTD profiles. Total precipitation was accumulated over the 1-, 6-, 12-, and 24-h windows before each uCTD profile, while wind stress magnitude was averaged over the same windows. Panels (a) and (b) show Pearson r and Spearman ρ correlations between BLT and total precipitation, and panels (c) and (d) show Pearson r and Spearman ρ correlations between BLT and wind stress. Values above or below the bars show the correlation coefficients, and p-values are shown within each panel.

Full correlation results, including wind speed and P − E, are provided in Table A3; profile-level 24-h forcing values are provided in Table A4.

Barrier Layer Thickness and Upper Ocean Heat Content

Upper-ocean heat content was calculated over the fixed 0–200 m layer for independent profiles with sufficient depth coverage. Of the 43 independent profiles, 42 extended to at least 200 dbar and were included in the primary OHC analysis. Profile ZW_11 was excluded because it reached only 159 dbar. Across the 42 profiles, $OHC_{0-200\,m}$ ranged from 21.04 to 22.25 $GJ\ m^{-2}$, while BLT ranged from 0.3 to 124.5 m (Table A5).

BLT showed a weak positive but not statistically significant relationship with $OHC_{0-200\,m}$ (Fig. 6). The Pearson correlation was r = 0.223 (p = 0.156), and the Spearman correlation was ρ = 0.253 (p = 0.105). These values indicate that profiles with thicker BLs tended to have slightly higher fixed-depth OHC, but the relationship was not statistically significant at the 0.05 level. The 10–200 m robustness check gave similar results, with Pearson r = 0.23 and Spearman ρ = 0.27, so excluding the uppermost 10 m did not substantially change the BLT–OHC relationship (Table A5).

The distribution of OHC also varied by transect group. Zonal West profiles generally occupied the lower OHC range, zonal East profiles covered a broader range, and meridional profiles were concentrated at higher OHC values (Figs. 6–7). Several meridional profiles had high OHC despite thin BLT, while several thick BL profiles did not have the highest OHC values. These profiles show that similar BLT values could occur with different OHC values, and similar OHC values could occur across different BLT ranges.

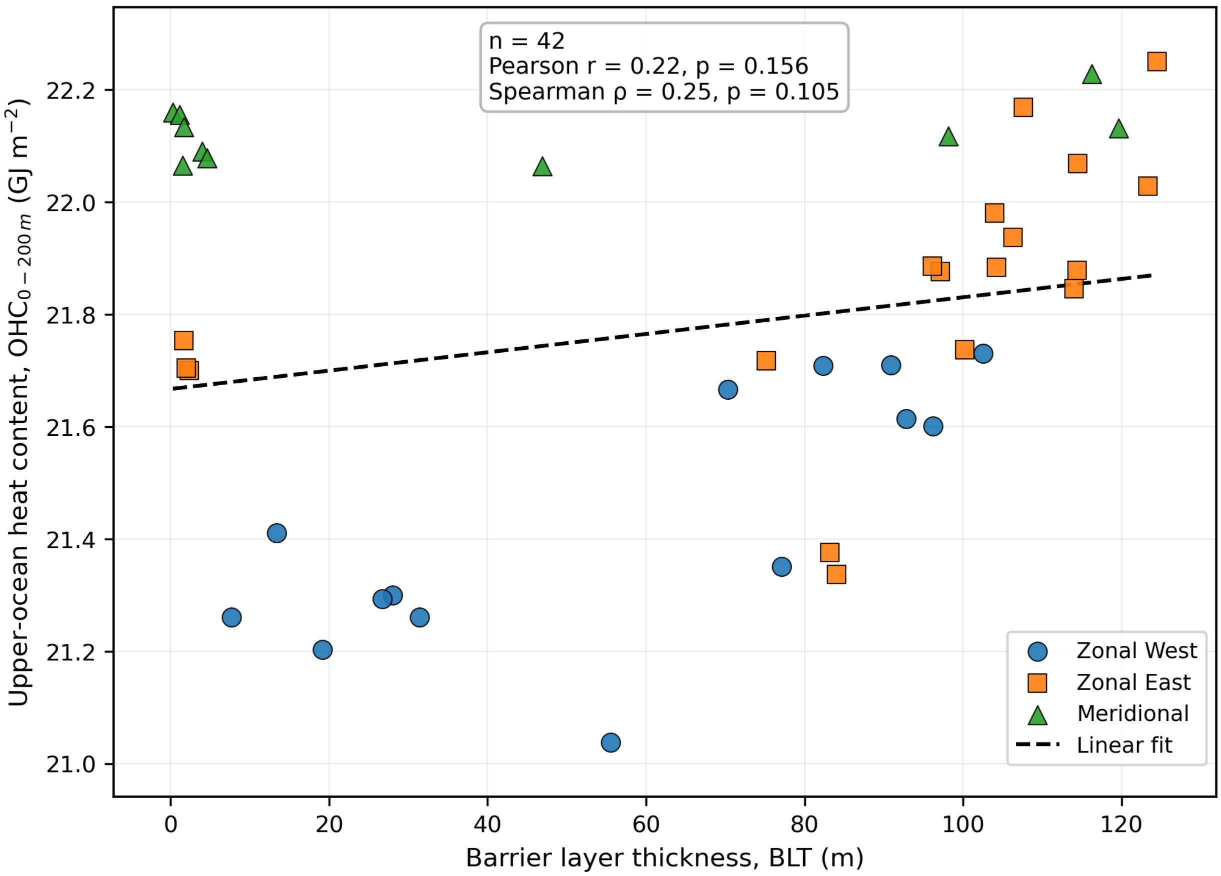

Figure 6. Relationship between BLT and OHC. BLT is plotted against upper-ocean heat content integrated over the fixed 0–200 m layer. Each point represents one independent uCTD profile with valid temperature coverage to at least 200 m. Points are colored by transect group. The dashed line shows the least-squares linear fit across all profiles. BLT showed a weak positive relationship with OHC_{0-200m}, but the correlation was not statistically significant across the full set of profiles.

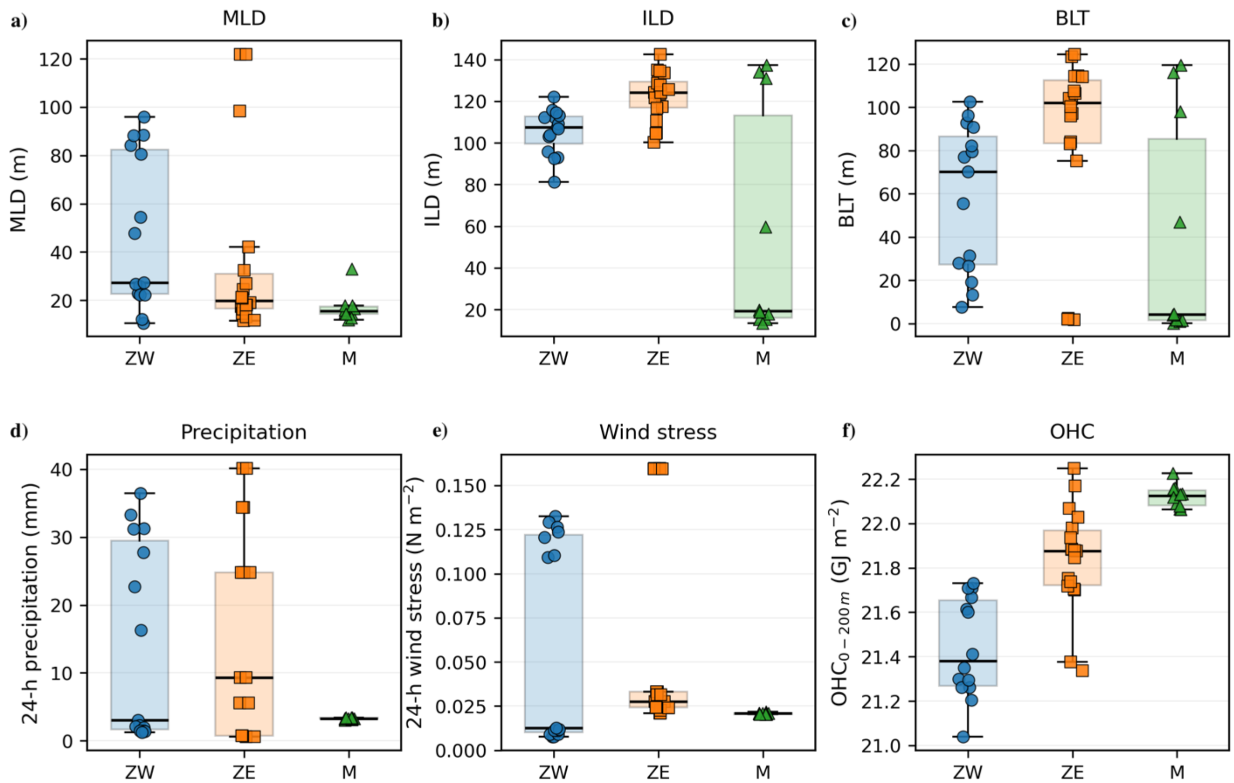

Figure 7. Transect-group comparison of upper-ocean structure, 24-h surface forcing, and upper-ocean heat content. Boxplots and individual points show the distribution of (a) MLD, (b) ILD, (c) BLT, (d) 24-h accumulated precipitation, (e) 24-h mean wind stress, and (f) OHC integrated over 0–200 m for the zonal West, zonal East, and meridional transects. Boxes indicate the interquartile range, central black lines indicate the median, whiskers show the non-outlier range, and points show individual independent uCTD profiles. OHC is shown for profiles with valid temperature coverage to at least 200 m; profile ZW_11 was excluded from the OHC panel because it did not reach 200 dbar.

Differences Between zonal Transects and meridional Transects

Transect-group comparisons show that upper-ocean structure, 24-h forcing, and OHC differed among the zonal West, zonal East, and meridional groups (Fig. 7). Zonal East had the thickest barrier layers overall, with a median BLT of 102.1 m. Zonal West had a lower median BLT of 70.3 m and included thin, moderate, and thick BL cases. The meridional group had the lowest median BLT of 4.3 m, but it also contained several thick BL profiles, showing a strong contrast within the same transect.

The structural variables also differed among transects. MLD was deepest and most variable in the zonal West transect, while zonal East had a shallower median MLD and the deepest median ILD. The meridional group had the shallowest and most tightly grouped MLD values but a wide ILD range because some profiles had very shallow ILDs and others had ILDs greater than 130 m (Fig. 7a–c; Table 1). These differences produced the large BLT contrasts among transects and within the meridional group.

Surface forcing varied most strongly in the two zonal transects. Zonal West and zonal East both showed large ranges in 24-h precipitation and wind stress, while meridional forcing values were more tightly clustered (Fig. 7d–e; Table A4). OHC increased from zonal West to zonal East to meridional profiles, but BLT did not increase in the same order (Fig. 7c, f). The meridional group had the highest and most tightly grouped OHC values even though many of its profiles had thin BLs. These transect-group patterns are consistent with the weak full-dataset BLT–OHC correlations reported above.

Discussion

Barrier Layer

The BLT results show that the sampled region contained spatially heterogeneous barrier layers and strong profile-scale stratification (Fig. 4; Table A1). In the thick BL profiles, MLD was much shallower than ILD, which is consistent with the classic definition of a barrier layer as the layer between the mixed layer and isothermal layer (Lukas & Lindstrom, 1991). This structure indicates that salinity stratification was strong enough to restrict density-defined vertical mixing even though warm water extended to greater depth.

The frequent occurrence of thick BLs in the zonal East transect is consistent with the broader western Pacific warm pool environment, where thick and seasonally varying barrier layers are commonly observed because salinity stratification can be strong (Bosc et al., 2009; Lukas & Lindstrom, 1991). However, the east–west difference observed in this study should not be interpreted as evidence for a single controlling mechanism. Thick BLs can form through multiple processes, including surface freshwater input, weak wind mixing, lateral advection of salinity fronts, and water-mass contrasts (Bosc et al., 2009; Katsura & Sprintall, 2020; Zhang et al., 2021). Therefore, the high BLT values on the east side of the Mariana Trench provide evidence of strong stratification during the sampling period, but they do not by themselves identify what produced that stratification.

The meridional transect shows that barrier-layer structure can change sharply over kilometer-scale distances. Profiles M_01–M_05 and M_10 were thin BL cases, while M_06–M_09 were thick BL cases (Fig. 3; Fig. A3; Table A1). This contrast was mainly associated with changes in ILD rather than large changes in MLD, suggesting that the depth of the warm layer varied strongly while the density-defined mixed layer generally remained shallow. One possible interpretation is that the transect crossed a sharp horizontal gradient in upper-ocean temperature or salinity structure, such as a small-scale front or water-mass boundary. However, because this study does not include direct current measurements or horizontal salinity-budget calculations, the origin of that gradient cannot be determined from the uCTD profiles alone.

Barrier layer thickness and surface forcing

Wind stress was the strongest recent surface-forcing signal associated with BLT, while precipitation-related variables showed weak relationships. The weak precipitation correlations do not mean that rainfall is unimportant for barrier layer formation in general. They indicate that, within this short cruise-based dataset, ERA5 precipitation over the previous 1–24 h did not explain the observed BLT variability. One possible reason is that the sampling period did not capture a sustained or spatially widespread heavy precipitation event near the profiles. Although short and localized rain occurred during the sampling period, such rainfall may not have been strong, long-lasting, or spatially aligned with the profile locations enough to produce a clear BLT signal in this dataset.

Another limitation is the scale mismatch between ERA5 precipitation and shipboard uCTD profiles. ERA5 represents precipitation over a gridded area and hourly time windows, while each uCTD profile samples a local water column at a specific time and location. Tropical rainfall can be patchy and short-lived, so gridded ERA5 values may smooth or miss rainfall that occurred directly over the ship track. In addition, the observed barrier layers may have been influenced by pre-existing salinity stratification rather than only by rainfall during the 1–24 h windows before each profile.

In contrast, wind stress showed the clearest statistical relationship with BLT. Pearson correlations between BLT and wind stress were negative and statistically significant for the 6-, 12-, and 24-h windows, with the strongest value over the 24-h window (Table A3; Fig. 5c). This pattern is physically consistent with the expectation that stronger wind stress can enhance turbulent mixing and reduce the separation between MLD and ILD, while weaker wind stress can allow salinity stratification to persist. However, this study did not directly measure turbulent mixing or follow the same water column through time, so the wind-stress result should be interpreted as a descriptive association rather than causal proof.

The weaker and non-significant Spearman correlations further show that the BLT–wind stress relationship was not a simple monotonic relationship across all profiles. Pearson correlation can be influenced by transect-group structure or by profiles with large BLT and low wind stress. Therefore, wind stress may have been one part of the observed BLT variability, along with pre-existing salinity stratification, horizontal advection, and local water-mass structure.

Barrier layer thickness and upper-ocean heat content

The relationship between BLT and upper-ocean heat content was weakly positive but not statistically significant (Fig. 6). It partially supports the initial hypothesis that thicker BLs may be associated with greater OHC, but it also shows that BLT alone did not explain fixed-depth OHC across the full dataset. This distinction is important because a barrier layer is expected to influence vertical heat redistribution and entrainment cooling, while OHC integrated over 0–200 m represents the total heat content of a much deeper fixed layer.

The weak positive BLT–OHC relationship is physically consistent with barrier-layer dynamics, even though it was not statistically significant. A thick barrier layer can reduce entrainment of cooler subsurface water into the mixed layer and help maintain warm upper-ocean conditions. This mechanism is consistent with the broader role of barrier layers in reducing vertical exchange between the mixed layer and thermocline waters (Lukas & Lindstrom, 1991; Bosc et al., 2009). However, the fixed 0–200 m OHC metric includes water above, within, and below the barrier layer. A profile can therefore have high OHC because the entire upper 200 m is warm, even if BLT is thin, and a thick BL does not necessarily imply the highest OHC over the full fixed-depth layer.

This helps explain why some meridional profiles had high OHC despite very thin BLT values (Figs. 6–7; Table A5). Those profiles suggest that high upper-ocean heat content can occur independently of a thick local barrier layer when the broader upper-ocean temperature field is warm. Conversely, some thick BL profiles did not have the highest OHC values. These patterns indicate that fixed-depth OHC depends not only on BLT but also on broader upper-ocean temperature structure, thermocline depth, and spatial position along the transects.

The similarity between the 0–200 m and 10–200 m OHC results suggests that the weak BLT–OHC relationship was not controlled only by the uppermost 10 m. Near-surface temperature can be affected by diurnal warming, short-term air–sea fluxes, and surface noise. However, removing the top 10 m did not substantially change the relationship, which supports the interpretation that the observed BLT–OHC pattern reflects broader upper-ocean structure rather than only a shallow surface signal.

Differences between zonal transects and meridional transects

The transect comparison helps explain why BLT and fixed-depth OHC were only weakly related. Zonal East had the thickest barrier layers overall, but the meridional group had the highest and most tightly grouped OHC values even though many meridional profiles had thin BLs (Fig. 7). This means that high OHC did not always occur in the same profiles or transect group as high BLT. The result is consistent with the definition of fixed-depth OHC: OHC integrated over 0–200 m reflects the temperature of the entire upper 200 m, while BLT only describes the vertical separation between the density-defined mixed layer and the temperature-defined isothermal layer.

The forcing comparison also needs to be interpreted in the context of transect differences. Zonal West and zonal East had wider ranges in 24-h precipitation and wind stress, while the meridional transect had more uniform forcing values (Fig. 7d–e; Table A4). Because the profiles were not evenly distributed in space and were collected over a short cruise period, some apparent relationships between forcing and BLT may partly reflect where the profiles were collected rather than only how each profile responded to recent local forcing. This is why the correlation results are treated as descriptive patterns rather than causal tests.

Several limitations affect the interpretation of this study. The uCTD sampling covered only a short cruise-based snapshot and did not resolve seasonal variability or time evolution of barrier layers. The spatial resolution was uneven, with sparse sampling along the zonal West transect and higher-resolution repeated profiles on the east side. In addition, ERA5 forcing is gridded, while uCTD profiles are local water-column measurements, which is especially important for short-lived and patchy tropical precipitation. Finally, fixed-depth OHC is not the same as heat content specifically within the mixed layer, within the barrier layer, or below the ILD.

Conclusions

The original hypothesis was that thicker barrier layers would be associated with greater upper-ocean heat content within a fixed-depth layer for this study. This hypothesis was partially supported but not statistically confirmed. The zonal East transect had the thickest and most persistent barrier layers, while the meridional transect showed the sharpest short-distance transition between thin and thick barrier layers. ERA5 surface forcing showed that precipitation was weakly related to BLT across the tested 1-, 6-, 12-, and 24-h windows. In contrast, wind stress showed a stronger negative Pearson correlation with BLT, especially over the 24-h window. However, because the Spearman correlations were weaker, this relationship should be interpreted as a descriptive pattern rather than direct causal evidence. BLT showed a weak positive relationship with $OHC_{0-200\ m}$, but the correlation was not statistically significant across the full dataset. Despite limitations from uneven uCTD sampling, the short cruise-based sampling window, and the mismatch between gridded ERA5 forcing and local profile measurements, this study shows that salinity-driven stratification near the Mariana Trench can produce thick and highly variable barrier layers, and that these structures may influence upper-ocean heat retention in the western tropical Pacific. Future work should separate heat content within the mixed layer, BL, and below the ILD to test the heat-retention mechanism more directly.

Acknowledgements

This work was supported by the University of Washington School of Oceanography through the 2026 Senior Cruise. I gratefully acknowledge the captain, crew, and marine technicians of the R/V *Thomas G. Thompson* for their support during the cruise from March 21 to April 1, 2026. I am also grateful to the professors, teaching staff, and classmates who worked in shifts to collect CTD and uCTD data during the cruise. Their effort and collaboration provided the observational foundation for this study. I especially thank Professor Alison Gray for her guidance, feedback, and support throughout the development of this senior thesis. AI use: Grammarly was used for grammar checking. ChatGPT was used for literature-search support, translation support for draft sentences, and feedback on sentence structure, redundancy, and clarity.

References

Benthuysen, J. A., Oliver, E. C. J., Feng, M., & Marshall, A. G. (2018). Extreme marine warming across tropical Australia during austral summer 2015–2016. Journal of Geophysical Research: Oceans, 123(2), 1301–1326. https://doi.org/10.1002/2017JC013326

Bosc, C., Delcroix, T., & Maes, C. (2009). Barrier layer variability in the western Pacific warm pool from 2000 to 2007. Journal of Geophysical Research: Oceans, 114, C06023. https://doi.org/10.1029/2008JC005187

Couch, C. S., Burns, J. H., Liu, G., Steward, K., Gutlay, T. N., Kenyon, J., Eakin, C. M., & Kosaki, R. K. (2017). Mass coral bleaching due to unprecedented marine heatwave in Papahānaumokuākea Marine National Monument (Northwestern Hawaiian Islands). PLOS ONE, 12(9), e0185121. https://doi.org/10.1371/journal.pone.0185121

de Boyer Montégut, C., Madec, G., Fischer, A. S., Lazar, A., & Iudicone, D. (2004). Mixed layer depth over the global ocean: An examination of profile data and a profile-based climatology. Journal of Geophysical Research: Oceans, 109, C12003. https://doi.org/10.1029/2004JC002378

Hersbach, H., Bell, B., Berrisford, P., Biavati, G., Horányi, A., Muñoz Sabater, J., Nicolas, J., Peubey, C., Radu, R., Rozum, I., Schepers, D., Simmons, A., Soci, C., Dee, D., & Thépaut, J.-N. (2023). ERA5 hourly data on single levels from 1940 to present. Copernicus Climate Change Service Climate Data Store. https://doi.org/10.24381/cds.adbb2d47

Hobday, A. J., Alexander, L. V., Perkins, S. E., Smale, D. A., Straub, S. C., Oliver, E. C. J., Benthuysen, J. A., Burrows, M. T., Donat, M. G., Feng, M., Holbrook, N. J., Moore, P. J., Scannell, H. A., Sen Gupta, A., & Wernberg, T. (2016). A hierarchical approach to defining marine heatwaves. Progress in Oceanography, 141, 227–238. https://doi.org/10.1016/j.pocean.2015.12.014

Katsura, S., & Sprintall, J. (2020). Seasonality and formation of barrier layers and associated temperature inversions in the eastern tropical North Pacific. Journal of Physical Oceanography, 50(3), 791–808. https://doi.org/10.1175/JPO-D-19-0194.1

Lukas, R., & Lindstrom, E. (1991). The mixed layer of the western equatorial Pacific Ocean. Journal of Geophysical Research: Oceans, 96(C2), 3343–3357. https://doi.org/10.1029/90JC01951

Zhang, X., Sprintall, J., & Zeng, L. (2021). What role does the barrier layer play during extreme El Niño events? Journal of Geophysical Research: Oceans, 126(5), e2020JC017001. https://doi.org/10.1029/2020JC017001

Appendix A: Additional uCTD Barrier Layer Results. This appendix provides profile-level BLT, duplicate-file screening, ERA5 forcing, OHC, and full-profile plotting results that support the main-text analyses.

Table A1. Full profile-level MLD, ILD, and BLT results for independent uCTD profiles.

Profile ID	Transect group	Source file	Max depth (m)	MLD (m)	ILD (m)	BLT (m)	BL class
ZW_01	zonal West	211495_20260324_0727_profile0.csv	255	80.6	112.1	31.4	thick BL (≥30 m)
ZW_02	zonal West	211495_20260324_0818_profile0.csv	247	47.7	103.2	55.5	thick BL (≥30 m)
ZW_03	zonal West	211495_20260324_0956_profile0.csv	251	88.4	107.6	19.2	moderate BL (10–30 m)
ZW_04	zonal West	211495_20260324_1050_profile0.csv	331	96	109.3	13.4	moderate BL (10–30 m)
ZW_05	zonal West	211495_20260324_1144_profile0.csv	338	84.3	112.3	28	moderate BL (10–30 m)
ZW_06	zonal West	211495_20260324_1344_profile0.csv	288	88.2	95.9	7.7	thin BL (<10 m)
ZW_07	zonal West	211495_20260324_1458_profile0.csv	255	54.4	81.2	26.7	moderate BL (10–30 m)
ZW_08	zonal West	211495_20260327_0515_profile0.csv	323	22.9	115.7	92.8	thick BL (≥30 m)
ZW_09	zonal West	211495_20260327_0515_profile1.csv	325	25.9	122.1	96.2	thick BL (≥30 m)
ZW_10	zonal West	211495_20260327_0703_profile0.csv	323	26.7	103.8	77.1	thick BL (≥30 m)
ZW_11	zonal West	211495_20260327_0703_profile1.csv	159	27.3	106.9	79.5	thick BL (≥30 m)
ZW_12	zonal West	211495_20260327_0853_profile0.csv	317	10.6	92.9	82.3	thick BL (≥30 m)
ZW_13	zonal West	211495_20260327_0853_profile1.csv	300	22.3	92.6	70.3	thick BL (≥30 m)
ZW_14	zonal West	211495_20260327_1034_profile0.csv	313	22.3	113.2	90.9	thick BL (≥30 m)
ZW_15	zonal West	211495_20260327_1034_profile1.csv	295	12.1	114.6	102.5	thick BL (≥30 m)
ZE_01	zonal East	211495_20260325_1520_profile0.csv	353	121.9	124.3	2.4	thin BL (<10 m)

Profile ID	Transect group	Source file	Max depth (m)	MLD (m)	ILD (m)	BLT (m)	BL class
ZE_02	zonal East	211495_20260325_1520_profile1.csv	259	121.8	123.4	1.7	thin BL (<10 m)
ZE_03	zonal East	211495_20260325_1520_profile2.csv	273	98.3	100.3	2	thin BL (<10 m)
ZE_04	zonal East	211495_20260325_1556_profile0.csv	310	42.1	117.3	75.2	thick BL (≥30 m)
ZE_05	zonal East	211495_20260326_1323_profile0.csv	262	32.4	129.5	97.1	thick BL (≥30 m)
ZE_06	zonal East	211495_20260326_1323_profile1.csv	267	24.6	128.6	104	thick BL (≥30 m)
ZE_07	zonal East	211495_20260326_1323_profile2.csv	279	17.4	121.6	104.2	thick BL (≥30 m)
ZE_08	zonal East	211495_20260326_1323_profile3.csv	270	19	133.5	114.5	thick BL (≥30 m)
ZE_09	zonal East	211495_20260326_1323_profile4.csv	286	11.6	134.9	123.3	thick BL (≥30 m)
ZE_10	zonal East	211495_20260326_1323_profile5.csv	248	14.5	110.5	96.1	thick BL (≥30 m)
ZE_11	zonal East	211495_20260326_1555_profile0.csv	273	16.4	116.7	100.2	thick BL (≥30 m)
ZE_12	zonal East	211495_20260326_1555_profile1.csv	268	18	124.3	106.3	thick BL (≥30 m)
ZE_13	zonal East	211495_20260327_1725_profile0.csv	326	27	134.6	107.6	thick BL (≥30 m)
ZE_14	zonal East	211495_20260327_1725_profile1.csv	280	18	142.5	124.5	thick BL (≥30 m)
ZE_15	zonal East	211495_20260327_1909_profile0.csv	332	13.2	127.6	114.4	thick BL (≥30 m)
ZE_16	zonal East	211495_20260327_1909_profile1.csv	304	11.7	125.7	114	thick BL (≥30 m)
ZE_17	zonal East	211495_20260327_2011_profile0.csv	329	20.8	104.7	84	thick BL (≥30 m)
ZE_18	zonal East	211495_20260327_2011_profile1.csv	313	21.2	104.4	83.2	thick BL (≥30 m)
M_01	meridional	stn67bcast1_profile0.csv	335	15	15.3	0.3	thin BL (<10 m)
M_02	meridional	stn67bcast1_profile1.csv	361	14.3	15.3	1.1	thin BL (<10 m)
M_03	meridional	stn67bcast2_profile0.csv	336	16.6	18.1	1.5	thin BL (<10 m)
M_04	meridional	stn67bcast2_profile1.csv	338	11.9	13.6	1.7	thin BL (<10 m)

Profile ID	Transect group	Source file	Max depth (m)	MLD (m)	ILD (m)	BLT (m)	BL class
M_05	meridional	stn67bcast2_profile2.csv	334	16	19.9	4	thin BL (<10 m)
M_06	meridional	stn67bcast2_profile3.csv	328	17.9	134.1	116.2	thick BL (≥30 m)
M_07	meridional	stn67bcast2_profile4.csv	327	33	131.1	98.1	thick BL (≥30 m)
M_08	meridional	stn67bcast2_profile5.csv	324	17.8	137.3	119.6	thick BL (≥30 m)
M_09	meridional	stn67bcast2_profile6.csv	319	12.8	59.7	46.9	thick BL (≥30 m)
M_10	meridional	stn67bcast2_profile7.csv	322	14.4	19	4.6	thin BL (<10 m)

Note: MLD, ILD, and BLT are defined in the Methods section. Values were calculated from independent uCTD profiles after duplicated or aliased processed files were screened to avoid counting the same physical profile more than once. Max depth refers to the maximum depth of the 1 m binned profile. Thin, moderate, and thick barrier layers are defined as BLT <10 m, 10–30 m, and ≥30 m, respectively. Profile IDs match those used in Figures 3, 4, and A1–A3.

Table A2. Recorded alias/duplicate mapping for processed uCTD profile files, filtered by comparing MLD, ILD, and BLT values.

Alias group	Transect group	Kept profile ID	Kept source file	Number of alias files	MLD (m)	ILD (m)	BLT (m)	All profile IDs	All source files
16	zonal East	ZE_01	211495_20260325_1520_profile0.csv	2	121.9	124.3	2.4	ZE_01; ZE_19	211495_20260325_1520_profile0.csv; stn_45_46_cast_1_profile0.csv
17	zonal East	ZE_02	211495_20260325_1520_profile1.csv	2	121.8	123.4	1.7	ZE_02; ZE_20	211495_20260325_1520_profile1.csv; stn_45_46_cast_1_profile1.csv
18	zonal East	ZE_03	211495_20260325_1520_profile2.csv	2	98.3	100.3	2	ZE_03; ZE_21	211495_20260325_1520_profile2.csv; stn_45_46_cast_1_profile2.csv
19	zonal East	ZE_04	211495_20260325_1556_profile0.csv	2	42.1	117.3	75.2	ZE_04; ZE_22	211495_20260325_1556_profile0.csv; stn_46_47_cast_1_profile0.csv
20	zonal East	ZE_05	211495_20260326_1323_profile0.csv	2	32.4	129.5	97.1	ZE_05; ZE_23	211495_20260326_1323_profile0.csv; stn_54_55_cast1_profile0.csv
21	zonal East	ZE_06	211495_20260326_1323_profile1.csv	2	24.6	128.6	104	ZE_06; ZE_24	211495_20260326_1323_profile1.csv; stn_54_55_cast1_profile1.csv
22	zonal East	ZE_07	211495_20260326_1323_profile2.csv	2	17.4	121.6	104.2	ZE_07; ZE_25	211495_20260326_1323_profile2.csv; stn_54_55_cast1_profile2.csv
23	zonal East	ZE_08	211495_20260326_1323_profile3.csv	2	19	133.5	114.5	ZE_08; ZE_26	211495_20260326_1323_profile3.csv; stn_54_55_cast1_profile3.csv
24	zonal East	ZE_09	211495_20260326_1323_profile4.csv	2	11.6	134.9	123.3	ZE_09; ZE_27	211495_20260326_1323_profile4.csv; stn_54_55_cast1_profile4.csv
25	zonal East	ZE_10	211495_20260326_1323_profile5.csv	2	14.5	110.5	96.1	ZE_10; ZE_28	211495_20260326_1323_profile5.csv; stn_54_55_cast1_profile5.csv

Alias group	Transect group	Kept profile ID	Kept source file	Number of alias files	MLD (m)	ILD (m)	BLT (m)	All profile IDs	All source files
26	zonal East	ZE_11	211495_20260326_1555_profile0.csv	2	16.4	116.7	100.2	ZE_11; ZE_29	211495_20260326_1555_profile0.csv; stn_55_56_cast1_profile0.csv
27	zonal East	ZE_12	211495_20260326_1555_profile1.csv	2	18	124.3	106.3	ZE_12; ZE_30	211495_20260326_1555_profile1.csv; stn_55_56_cast1_profile1.csv

Note: This table lists processed uCTD profile files that were treated as duplicated or aliased files. Alias files were identified when profiles within the same transect group had identical maximum binned depth, MLD, ILD, and BLT values after rounding to 0.1 m. These matches indicate that the same physical profile was likely saved under both timestamp-based and station-based filenames. Only the kept profile ID was retained for the main BLT analysis to avoid counting the same physical profile more than once.

Table A3. Pearson r, Pearson p-value, Spearman ρ, and Spearman p-value for correlations between BLT and ERA5-derived surface forcing variables across four forcing windows.

Forcing variable	Window	n	Pearson r	Pearson p	Spearman ρ	Spearman p
Total precipitation	1 h	43	0.209	0.179	-0.084	0.591
Total precipitation	6 h	43	0.027	0.862	-0.153	0.327
Total precipitation	12 h	43	0.015	0.924	-0.06	0.701
Total precipitation	24 h	43	-0.004	0.98	-0.134	0.391
P − E	1 h	43	0.212	0.172	-0.096	0.54
P − E	6 h	43	0.037	0.813	-0.156	0.319
P − E	12 h	43	0.034	0.827	-0.125	0.423
P − E	24 h	43	0.049	0.755	-0.084	0.594
Wind speed	1 h	43	-0.111	0.479	-0.029	0.856
Wind speed	6 h	43	-0.197	0.206	-0.023	0.882
Wind speed	12 h	43	-0.28	0.069	-0.009	0.954
Wind speed	24 h	43	-0.436	0.003	-0.148	0.343
Wind stress	1 h	43	-0.266	0.084	-0.059	0.705
Wind stress	6 h	43	-0.462	0.002	-0.171	0.272
Wind stress	12 h	43	-0.462	0.002	-0.071	0.651
Wind stress	24 h	43	-0.524	<0.001	-0.187	0.231

Note: Correlations were calculated between BLT and ERA5-derived surface forcing variables for 43 independent uCTD profiles. Pearson r describes linear association, while Spearman ρ describes rank-based monotonic association. P-values are two-sided.

Total precipitation and P − E were accumulated over each window before the profile time, while wind speed and wind stress were averaged over the same windows.

Table A4. Calculated ERA5-matched 24-h time window surface forcing values for all uCTD profiles.

Profile	**Transect group**	**BLT (m)**	**24-h precipitation (mm)**	**24-h P − E (mm)**	**24-h mean wind speed ($m\ s^{-1}$)**	**24-h mean wind stress ($N\ m^{-2}$)**
ZW_01	zonal West	31.4	16.27	10.81	9.02	0.1326
ZW_02	zonal West	55.5	22.74	17.39	8.95	0.1293
ZW_03	zonal West	19.2	27.74	22.48	8.87	0.1264
ZW_04	zonal West	13.4	31.3	26.12	8.73	0.1236
ZW_05	zonal West	28	33.3	28.19	8.6	0.1207
ZW_06	zonal West	7.7	31.22	26.29	8.32	0.1094
ZW_07	zonal West	26.7	36.44	31.61	8.34	0.1104
ZW_08	zonal West	92.8	3.07	1.29	2.31	0.0078
ZW_09	zonal West	96.2	2.25	0.45	2.11	0.0076
ZW_10	zonal West	77.1	2.11	0.27	2.37	0.0091
ZW_11	zonal West	79.5	1.94	0.07	2.27	0.0091
ZW_12	zonal West	82.3	1.44	-0.56	2.62	0.0112
ZW_13	zonal West	70.3	1.44	-0.56	2.62	0.0112
ZW_14	zonal West	90.9	1.4	-0.69	2.86	0.0118
ZW_15	zonal West	102.5	1.25	-0.88	3.04	0.0126
ZE_01	zonal East	2.4	9.31	3.76	10.11	0.1598
ZE_02	zonal East	1.7	9.31	3.76	10.11	0.1598

Profile	Transect group	BLT (m)	24-h precipitation (mm)	24-h P − E (mm)	24-h mean wind speed (m s⁻¹)	24-h mean wind stress (N m⁻²)
ZE_03	zonal East	2	5.56	0.03	10.02	0.1594
ZE_04	zonal East	75.2	5.56	0.03	10.02	0.1594
ZE_05	zonal East	97.1	24.78	22.26	4.49	0.0276
ZE_06	zonal East	104	24.78	22.26	4.49	0.0276
ZE_07	zonal East	104.2	24.78	22.26	4.49	0.0276
ZE_08	zonal East	114.5	24.78	22.26	4.49	0.0276
ZE_09	zonal East	123.3	34.41	31.79	4.7	0.0332
ZE_10	zonal East	96.1	34.41	31.79	4.7	0.0332
ZE_11	zonal East	100.2	40.17	37.5	4.65	0.0315
ZE_12	zonal East	106.3	40.17	37.5	4.65	0.0315
ZE_13	zonal East	107.6	0.57	-2.17	3.84	0.0211
ZE_14	zonal East	124.5	0.57	-2.17	3.84	0.0211
ZE_15	zonal East	114.4	0.59	-2.23	3.91	0.0226
ZE_16	zonal East	114	0.61	-2.28	3.99	0.0241
ZE_17	zonal East	84	0.74	-2.11	4.12	0.0244
ZE_18	zonal East	83.2	0.74	-2.11	4.12	0.0244
M_01	meridional	0.3	3.03	0.38	2.95	0.0208
M_02	meridional	1.1	3.11	0.39	3.02	0.0217
M_03	meridional	1.5	3.28	0.59	2.95	0.021

Profile	Transect group	BLT (m)	24-h precipitation (mm)	24-h P − E (mm)	24-h mean wind speed (m s⁻¹)	24-h mean wind stress (N m⁻²)
M_04	meridional	1.7	3.28	0.59	2.95	0.021
M_05	meridional	4	3.28	0.59	2.95	0.021
M_06	meridional	116.2	3.28	0.59	2.95	0.021
M_07	meridional	98.1	3.28	0.59	2.95	0.021
M_08	meridional	119.6	3.42	0.74	2.85	0.0203
M_09	meridional	46.9	3.42	0.74	2.85	0.0203
M_10	meridional	4.6	3.42	0.74	2.85	0.0203

Note: This table provides the profile-level BLT and ERA5-matched 24-h forcing values used to support the surface-forcing analysis. Precipitation and P − E are accumulated over the 24 h before each profile, while wind speed and wind stress are averaged over the same period. Definitions of the forcing windows and correlation metrics are provided in Table A3.

Table A5. Profile-level upper-ocean heat content and barrier layer thickness for independent uCTD profiles.

Profile	Transect group	BLT (m)	Max depth (dbar)	OHC 0-200 m (GJ m⁻²)	OHC 10-200 m (GJ m⁻²)	OHC status
ZW_01	zonal West	31.4	255	21.26	20.127	ok
ZW_02	zonal West	55.5	247	21.038	19.905	ok
ZW_03	zonal West	19.2	251	21.203	20.072	ok
ZW_04	zonal West	13.4	331	21.411	20.279	ok
ZW_05	zonal West	28	338	21.3	20.169	ok
ZW_06	zonal West	7.7	288	21.261	20.131	ok
ZW_07	zonal West	26.7	255	21.294	20.167	ok
ZW_08	zonal West	92.8	323	21.614	20.469	ok
ZW_09	zonal West	96.2	325	21.601	20.458	ok
ZW_10	zonal West	77.1	323	21.351	20.205	ok
ZW_11	zonal West	79.5	159			excluded
ZW_12	zonal West	82.3	317	21.708	20.564	ok
ZW_13	zonal West	70.3	300	21.667	20.523	ok
ZW_14	zonal West	90.9	313	21.71	20.565	ok
ZW_15	zonal West	102.5	295	21.731	20.58	ok
ZE_01	zonal East	2.4	353	21.701	20.557	ok
ZE_02	zonal East	1.7	259	21.754	20.611	ok
ZE_03	zonal East	2	273	21.704	20.561	ok
ZE_04	zonal East	75.2	310	21.717	20.574	ok
ZE_05	zonal East	97.1	262	21.876	20.734	ok
ZE_06	zonal East	104	267	21.98	20.839	ok
ZE_07	zonal East	104.2	279	21.884	20.743	ok
ZE_08	zonal East	114.5	270	22.068	20.928	ok

Profile	Transect group	BLT (m)	Max depth (dbar)	OHC 0-200 m (GJ m⁻²)	OHC 10-200 m (GJ m⁻²)	OHC status
ZE_09	zonal East	123.3	286	22.028	20.886	ok
ZE_10	zonal East	96.1	248	21.886	20.743	ok
ZE_11	zonal East	100.2	273	21.737	20.596	ok
ZE_12	zonal East	106.3	268	21.937	20.796	ok
ZE_13	zonal East	107.6	326	22.169	21.026	ok
ZE_14	zonal East	124.5	280	22.25	21.104	ok
ZE_15	zonal East	114.4	332	21.878	20.729	ok
ZE_16	zonal East	114	304	21.846	20.691	ok
ZE_17	zonal East	84	329	21.337	20.189	ok
ZE_18	zonal East	83.2	313	21.377	20.222	ok
M_01	meridional	0.3	335	22.161	21	ok
M_02	meridional	1.1	361	22.156	21.001	ok
M_03	meridional	1.5	336	22.066	20.905	ok
M_04	meridional	1.7	338	22.134	20.972	ok
M_05	meridional	4	334	22.09	20.931	ok
M_06	meridional	116.2	328	22.228	21.073	ok
M_07	meridional	98.1	327	22.118	20.965	ok
M_08	meridional	119.6	324	22.131	20.979	ok
M_09	meridional	46.9	319	22.064	20.909	ok
M_10	meridional	4.6	322	22.079	20.925	ok

Note: OHC was integrated over fixed 0–200 m and 10–200 m layers. Profile ZW_11 did not reach 200 dbar and was excluded from the primary 0–200 m OHC correlation analysis. Blank OHC values indicate insufficient depth coverage.

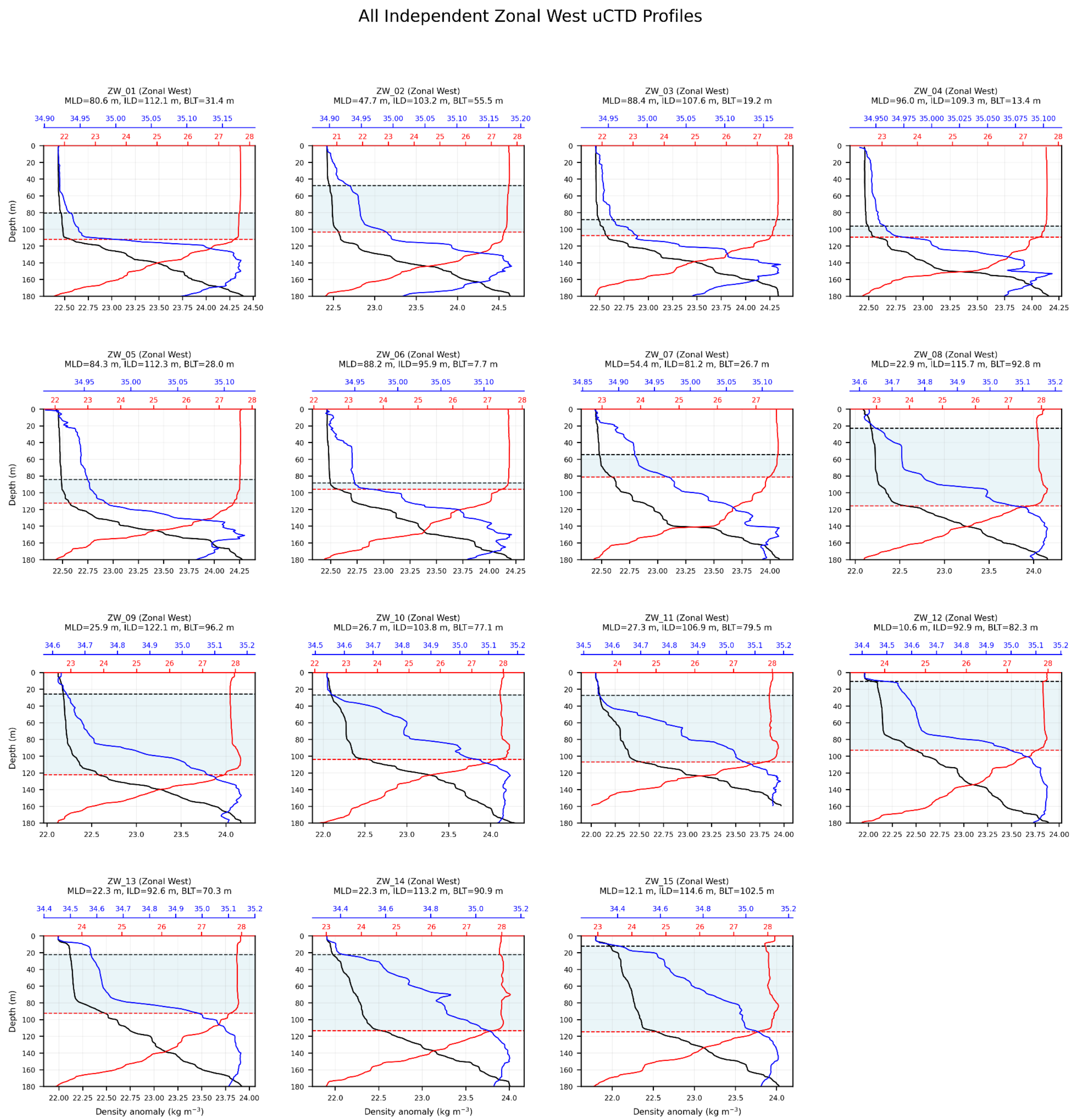

Figure A1. Full set of independent zonal West uCTD profiles with calculated BLT. Black curves show density anomaly, red curves show temperature, and blue curves show salinity. Black dashed lines mark MLD, red dashed lines mark ILD, and blue shading marks the barrier layer.

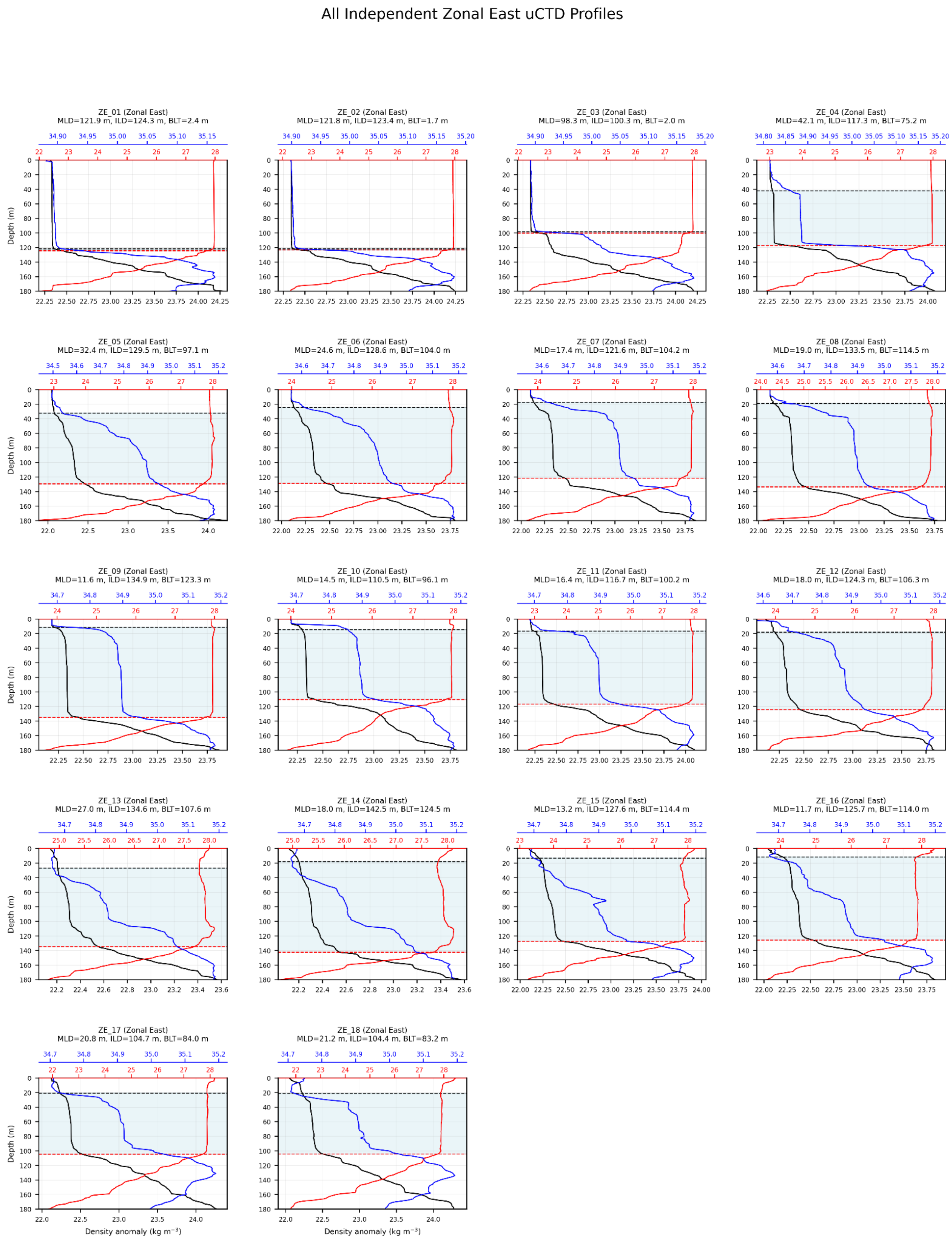

Figure A2. Full set of independent zonal East uCTD profiles with calculated BLT. Same plotting conventions as Figure A1.

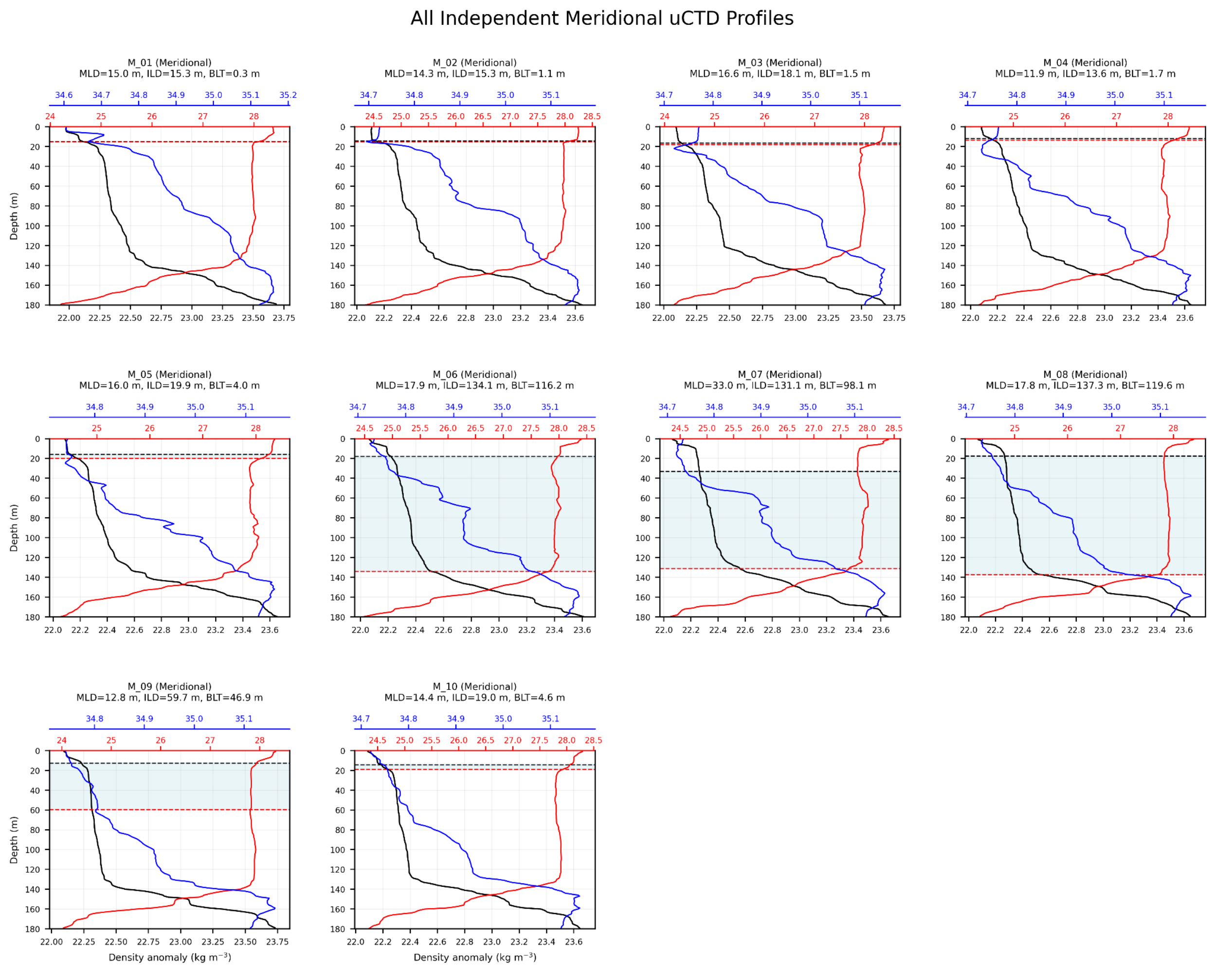

Figure A3. Full set of independent meridional uCTD profiles with calculated BLT. Same plotting conventions as Figure A1.